A Computed Tomography Scan Assessment of Regional Lung Volume in Acute Lung Injury

LOUIS PUYBASSET, PHILIPPE CLUZEL, NAN CHAO, ARTHUR S. SLUTSKY, PIERRE CORIAT, JEAN-JACQUES ROUBY, and the CT Scan ARDS Study Group

Unité de Réanimation Chirurgicale, Department of Anesthesiology and Department of Radiology (Thoracic Division), La Pitié-Salpêtrière Hospital, University of Paris VI, Paris, France; and Department of Medicine and Pathology, Mount Sinai Hospital, University of Toronto, Toronto, Canada

The lobar and cephalocaudal distribution of aerated and nonaerated lung and of PEEP-induced alveolar recruitment is unknown in acute lung injury (ALI). Dimensions of the lungs and volumes of aerated and nonaerated parts of each pulmonary lobe were measured using a computerized tomographic quantitative analysis and compared between 21 patients with ALI and 10 healthy volunteers. Distribution of PEEP-induced alveolar recruitment along the anteroposterior and cephalocaudal axis and influence of the resting volume of nonaerated lower lobes were also assessed. Anteroposterior and transverse dimensions of the lungs of the patients were similar to those of healthy volunteers, whereas cephalocaudal dimensions were reduced by more than 15%. Total lung volume (aerated plus nonaerated lung) was reduced by 27%. Volumes of upper and lower lobes were 99 and 48% of normal values. In addition to an anteroposterior gradient in the distribution of aerated and nonaerated areas, a cephalocaudal gradient was also observed. Nonaerated areas were predominantly found in juxtadiaphragmatic regions. PEEP-induced alveolar recruitment was more pronounced in nondependent than in dependent regions and in cephalad than in caudal regions. A significant correlation between resting volume of nonaerated lower lobes and regional PEEP-induced alveolar recruitment was observed. In ALI, loss of lung volume involves predominantly lower lobes. The thorax shortens along its cephalocaudal axis. PEEP-induced alveolar recruitment predominates in nondependent and cephalad lung regions and is inversely correlated with the resting volume of nonaerated lung. Puybasset L, Cluzel P, Chao N, Slutsky AS, Coriat P, Rouby J-J, and the CT Scan ARDS Study Group. A computed tomography scan assessment of regional lung volume in acute lung injury.

AM J RESPIR CRIT CARE MED 1998;158:1644–1655.

Loss of aerated lung volume is a characteristic feature of acute lung injury (ALI) and is commonly observed after major thoracic and abdominal surgical procedures. Reduction in lung volume is generally assessed by measuring FRC, using gas dilution techniques such as nitrogen (1) or sulfur hexafluoride (2, 3) washout and open- and closed-circuit helium dilution techniques (1, 4). These methods have the advantage of being noninvasive, allowing bedside and repeated measurements. However, they are not always reproducible (1, 2, 5) and do not provide any measurement of the volume of nonaerated lung. Furthermore, there are some important limitations common to all these techniques when applied to patients with ALI: (*1*) the diseased lung is characterized by the presence of poorly aerated areas where the gas mixing is problematic, (*2*) distention of previously aerated regions cannot be distinguished from true alveolar recruitment when FRC increases after positive end-expiratory pressure (PEEP), and (*3*) regional distribution of aerated and nonaerated lung volumes and of PEEP-induced alveolar recruitment cannot be assessed.

Chest computerized tomography (CT scan) is a technique that can overcome some of the limitations of these methods. By measuring lung densities, well-aerated regions can be easily differentiated from poorly and nonaerated lung regions. In patients critically ill with ALI, it has been demonstrated that lung hyperdensities predominate in the dependent regions (3, 6, 7). The superimposed hydrostatic pressure resulting from the edematous lung along an anteroposterior axis has been proposed to be a likely explanation for this regional distribution gradient (8, 9). Similarly, PEEP-induced alveolar recruitment has been shown to depend upon an anteroposterior gradient, the most dependent lung regions being less likely to be

(*Received in original form February 3, 1998 and in revised form July 6, 1998*)

The following members of the CT Scan ARDS Study Group participated in this study: T. E. Stewart, M.D., Ewart Angus ICU, Wellesley Hospital, Toronto Canada; P. Grenier, M.D., and S. Zaim, M.D., Department of Radiology, La Pitié-Salpêtrière Hospital, Paris, France; L. Gallart, M.D., and M. Puig, M.D., Servei d'Anestesiologia, Hospital Universitari del Mar, Barcelona, Spain; G. S. Umamaheswara Rao, M.D., Department of Anesthesia, National Institute of Mental Health and Neurosciences, Bengalore, India; J. Richecoeur, Réanimation Médicale Polyvalente, Pontoise, France; S. Vieira, M.D., Hospital de Clinicas de Porto Allegre, UFRGS, Brazil; and Q. Lu, M.D., Unité de Réanimation Chirurgicale, Hôpital de La Pitié-Salpêtrière, Paris, France.

Presented in part at the annual meeting of the European Society of Anesthesiology, London, United Kingdom, June 1996 and at the Annual Meeting of the American Thoracic Society, New Orleans, Louisiana, May 1996.

Correspondence and requests for reprints should be addressed to Dr. L. Puybasset, Surgical Intensive Care Unit, Department of Anesthesiology, La Pitié-Salpêtière Hospital, 47-83, Boulevard de l'Hôpital, 75013 Paris, France.

Am J Respir Crit Care Med Vol 158. pp 1644–1655, 1998
Internet address: www.atsjournals.org

TABLE 1

CLINICAL CHARACTERISTICS OF THE PATIENTS

Patient No.	Age (*yr*)	Sex	Cause of ALI	Surgical Incision	Outcome	SAPS	ASA	LISS	Ventilation Duration (*d*)	ICU Duration (*d*)
1	70	M	BPN	NTNA	S	19	2	1.5	22	18
2	72	F	BPN	NTNA	D	16	2	3.75	102	102
3	35	M	PC	THO/ABD	S	10	1	2.25	25	29
4	69	M	BPN	THO	S	13	3	3.0	37	34
5	50	F	AP	NTNA	S	11	2	2.25	39	43
6	46	M	BPN	ABD	D	18	3	1.7	26	25
7	38	M	Pancreatitis	NTNA	D	19	2	3.5	28	15
8	44	F	BPN	NTNA	D	8	1	3.0	37	36
9	71	M	BPN	THO/ABD	S	14	3	3.25	36	44
10	66	M	BPN	NTNA	D	20	2	3.25	24	16
11	45	M	BPN	THO	S	14	2	2.5	26	33
12	34	M	BPN	ABD	S	15	1	2.5	76	107
13	70	M	BPN	NTNA	S	11	3	2.0	20	20
14	43	M	BPN	NTNA	S	13	1	1.25	69	129
15	64	M	BPN	NTNA	S	16	2	2.25	48	48
16	69	F	SS	ABD	D	12	3	3.0	36	31
17	66	M	BPN	ABD	S	18	3	2.0	13	18
18	81	M	AP	NTNA	S	15	3	2.75	32	35
19	20	M	PC	NTNA	S	10	1	3.25	31	22
20	61	M	BPN	NTNA	D	10	3	3.5	14	7
21	40	F	SS	ABD	D	14	1	3.0	13	11
Mean						14.1	2.1	2.6	36	39
SD						3.4	0.8	0.7	22	33

Definition of abbreviations: ABD = abdominal; ALI = acute lung injury; AP = aspiration pneumonia; ASA = Score of the American Society of Anesthesiology; BPN = nosocomial pneumonia; D = deceased; LISS = lung injury severity score; NTNA = nonthoracic and nonabdominal; PC = pulmonary contusion; S = survived; SAPS = simplified acute physiological score; SS = septic shock; THO = thoracic.

recruited by PEEP than the nondependent lung regions (10). Because these different studies were performed using a limited number of CT sections (one to three), measurements of the volume of the entire lung and of each pulmonary lobe and assessment of the cephalocaudal distribution of lung consolidations could not be performed. The present study was undertaken to quantify lung volume loss and to assess its lobar distribution in patients with ALI. In addition, PEEP-induced alveolar recruitment and its anteroposterior and cephalocaudal distribution were studied after obtaining contiguous thoracic CT sections from the apex to the diaphragm with and without PEEP.

TABLE 2

RESPIRATORY CHARACTERISTICS OF THE PATIENTS

Patient No.	% Well Aerated	% Poorly Aerated	% Nonaerated	Cst (*ml/cm H_2O*)	Pop (*cm H_2O*)	Pa_{O_2} (*mm Hg*)	$\overline{Ppa}$ (*mm Hg*)	$\dot{V}_{DA}/V_T$ (%)
1	77	2	21	77	5	159	22	33
2	1	68	31	43	6	197	24	ND
3	23	47	30	36	ABS	81	27	18
4	82	11	7	50	6	104	43	35
5	48	20	33	42	6	69	21	35
6	60	22	19	38	4	90	53	ND
7	0	66	34	32	6	49	17	ND
8	35	37	27	37	7	77	25	36
9	67	9	24	64	3	58	39	ND
10	17	47	36	29	7	39	36	44
11	29	44	27	40	5	249	22	ND
12	8	55	37	35	10	115	31	50
13	0	75	25	60	ABS	111	41	33
14	59	16	26	54	3	82	18	27
15	16	34	50	28	ABS	73	49	32
16	2	51	47	44	ABS	79	33	47
17	31	47	21	87	5	247	22	42
18	36	17	47	63	4	125	34	42
19	9	31	59	34	9	76	41	51
20	38	7	54	30	6	59	45	33
21	8	60	32	22	10	50	35	67
Mean	31	36	33	45	6	104	32	39
SD	26	22	13	17	2	60	11	11

Definition of abbreviations: ABS = absent; Cst = quasi-static compliance; Pop = opening pressure determined after subtraction of intrinsic-PEEP; $\overline{Ppa}$ = mean pulmonary artery pressure; $\dot{V}_{DA}/V_T$ = alveolar dead space to tidal volume.

METHODS

Patients

Twenty-one consecutive hypoxemic patients with ALI diagnosed on or after admission to the Surgical Intensive Care Unit of La Pitié-Salpêtrière Hospital in Paris (Department of Anesthesiology) were included in a prospective study during the first 10 d of their acute respiratory disease. All of them were transported to the Department of Radiology and underwent a thoracic CT scan after informed consent had been obtained from their next of kin. Sixteen patients had their CT scans performed as they were enrolled in prospective studies on inhaled NO. The description of the CT scan procedure and of the risks of the transportation were clearly mentioned in the document accompanying the inform consent that was signed by the families. The clinical and radiologic characteristics of these patients have been reported in previously published articles (11–13). For the five remaining patients who were not included in studies on inhaled NO, complete explanations about the CT scan procedures were given to the families, and inform consent was obtained from all of them before inclusion in the study. Inclusion criteria were: (*1*) bilateral opacities on a bedside chest radiograph, (*2*) $Pa_{O_2} < 250$ mm Hg at an FI_{O_2} of 1.0 and zero end-expiratory pressure (ZEEP). Exclusion criteria were (*1*) cardiogenic pulmonary edema defined as a pulmonary capillary wedge pressure > 18 mm Hg and a left ventricular ejection fraction < 50% as estimated by a bedside transesophageal echocardiography, and (*2*) the presence of a bronchopleural fistula.

All the patients were sedated and paralyzed with a continuous intravenous infusion of fentanyl 250 μg/h, flunitrazepam 1 mg/h, and vecuronium 4 mg/h and ventilated using controlled mechanical ventilation (César Ventilator; Taema, Antony, France). An inspiratory time of 30% and an FI_{O_2} of 1 were maintained throughout the study period. All patients were monitored using a fiberoptic thermodilution pulmonary artery catheter (Baxter Healthcare Co., Irvine, CA) and a radial or femoral arterial catheter.

High Resolution and Spiral Thoracic CT Scan

As previously described (11–13), lung scanning was performed from the apex to the diaphragm using a Tomoscan SR 7000 (Philips, Eindhoven, The Netherlands). All images were observed and photographed at a window width of 1,600 HU and a level of −700 HU. An intravenous injection of 60 ml of contrast material was administered to each patient to differentiate pleural fluid collections from consolidated lung parenchyma. Evaluation included thin-section CT and spiral CT in all patients. The thin-section CT examination consisted of a series of sections 1.5 mm thick with 20-mm intersection spacing selected by means of a thoracic scout view during a 25-s period of apnea, the paralyzed patient being disconnected from the ventilator (pulmonary volume equal to apneic FRC, ZEEP). For spiral CT, contiguous axial sections 10 mm thick were reconstructed from the volumetric data obtained during a 15-s apnea. A PEEP of 10 cm H_2O was then applied for 15 min during controlled mechanical ventilation. The same CT scan protocol (thin-section and spiral CT) was repeated at an end-expiratory pressure of 10 cm H_2O by clamping the endotracheal tube connector at end-expiration (pulmonary volume equal to FRC after PEEP administration). Airway pressure was continuously monitored to ensure that a PEEP value of 10 cm H_2O was maintained during the CT acquisition. Mechanical ventilation was provided using an Osiris ventilator (Taema) specifically designed for transportation of critically ill patients and delivering 100% oxygen. Cardiovascular monitoring was performed using a Propaq 104 EL monitor (Protocol System, Beaverton, OR), allowing the continuous monitoring of pulse oximetry, systemic arterial pressure, and electrocardiogram. All the CT scans were performed with the patients in the supine position.

A spiral thoracic CT scan consisting of contiguous axial sections 10 mm thick was also performed at end-expiration in 10 spontaneously breathing healthy volunteers.

Volumetric Analysis of the Thoracic CT Scan

The aim of this analysis was to measure the volumes (gas plus tissue) and the anteroposterior and cephalocaudal distribution of the different lung zones—aerated, poorly aerated, and nonaerated—in ZEEP and PEEP conditions. Lung parenchyma was manually delineated by

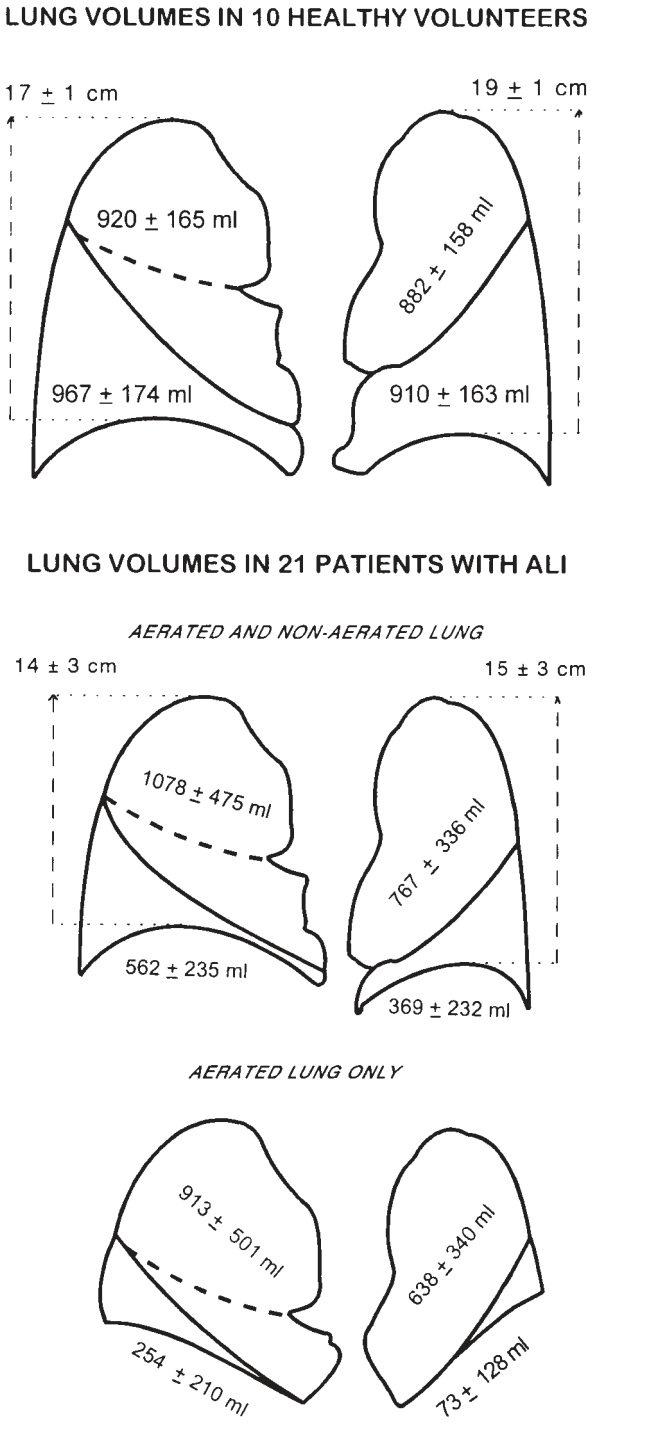

Figure 1. From the *upper* to the *lower* part of the figure: volumes of upper and lower lobes and cephalocaudal dimensions of right and left lungs obtained from the 10 healthy volunteers; volumes of upper and lower lobes and cephalocaudal dimensions of right and left lungs obtained from the 21 patients with acute lung injury; and volumes of normally and poorly aerated areas of upper and lower lobes obtained from the 21 patients with acute lung injury. All volumes and dimensions were measured at zero end-expiratory pressure. Each lung is drawn in profile. The oblique fissura is represented by the *continuous line* and the horizontal fissura is represented by the *dashed line*.

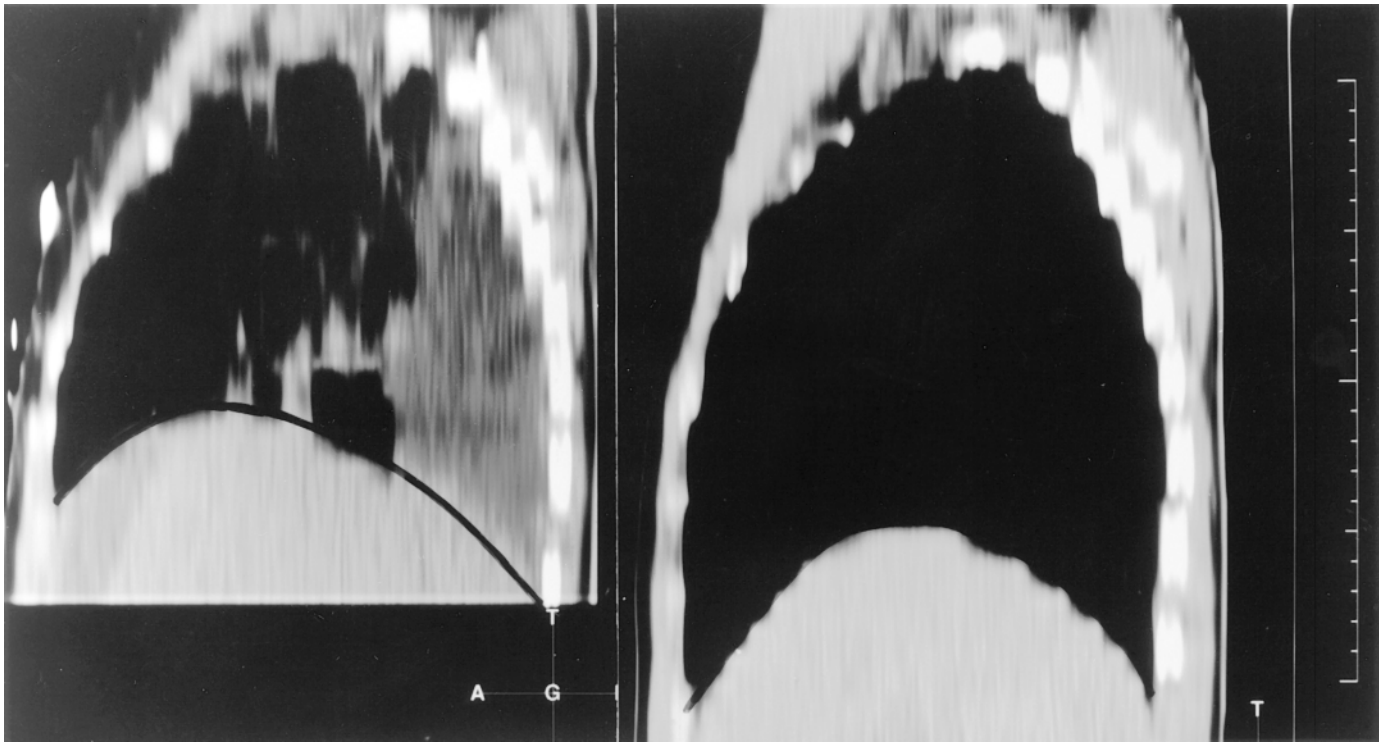

Figure 2. Sagittal reconstructions of the right lung (mediastinal windows) obtained from the contiguous CT sections in one patient with acute lung injury (*left side*) and one healthy volunteer (*right side*). The centimetric scale on the right side has a height of 20 cm.

one of the investigators (P.C.) after marking mediastinal structures and pleural effusion. Upper and lower lobes were delineated after fissures had been precisely identified on the thin sections. A specially designed transparent grid that had a between-line distance fitted to the 1-cm scale of the CT scan image was applied to each CT section from the apical to the diaphragmatic sections. As the thickness of each volumetric CT section was 1 cm and each square of the grid represented a surface of lung parenchyma of 1 cm^2, each square represented a lung volume of 1 cm^3. The first line of the grid was applied to each CT section in order to precisely fit the anterior margin of lung parenchyma. The total number of squares was determined for each line from the anterior to the posterior lung region. In order to measure the respective lung volumes of aerated, poorly aerated, and nonaerated lung areas, the radiologic density of each square of the grid was visually assessed by comparing its aspect to the gray scale of the CT scan and classified in one of the three categories proposed by Gattinoni and colleagues (6): areas corresponding to a density between −1,000 and −500 HU were considered as well aerated, areas corresponding to a density between −500 and −100 HU were considered as poorly aerated, and areas corresponding to a density between −100 and +100 HU were considered as nonaerated. This analysis was performed separately for upper and lower lobes. Because the right middle lobe could not easily be distinguished from the right upper lobe, it was considered as a part of the right upper lobe for the regional volume analysis. The amount of pleural fluid was also determined. As the volumetric analysis was performed in ZEEP and PEEP conditions, changes in lung volumes induced by PEEP could be precisely measured. PEEP-induced alveolar recruitment was calculated as the difference between the volume of nonaerated tissue in ZEEP minus the volume of nonaerated tissue in PEEP. Percentage of PEEP-induced alveolar recruitment was calculated as the volume recruited divided by the volume of nonaerated lung. A patient was arbitrarily defined as a "recruiter" if PEEP reduced the volume of nonaerated tissue by more than 10%; otherwise the patient was considered a "nonrecruiter."

The mean of the individual difference between two observers was 3 ± 158 ml for total lung volume and 2 ± 11 ml for pleural effusion volume measurements (n = 8). Intraobserver differences were 15 ± 75 and 7 ± 9 ml, respectively (n = 6).

The cephalocaudal dimension of each lung was determined as the number of sections 1 cm thick present between the lung apex and the dome of the diaphragmatic cupola. Transverse and anteroposterior dimensions were determined at the level of the tracheal carina using the length scale of the CT scan. For each patient, a sagittal section of the right lung was reconstructed from contiguous CT sections. Reconstruction was performed at the maximal convexity of the right diaphragmatic cupola analyzed on the frontal scout view.

Volumes of right and left upper and lower lobes and cephalocaudal, transverse, and anteroposterior distances were also measured in the 10 healthy volunteers at end-expiration. These measurements were performed to determine normal values of the lung dimensions and volumes.

Hemodynamic Measurements

Hemodynamic and respiratory variables in ZEEP and 15 min after administration of PEEP were measured within the 24 h before or after the CT scan in patients with ALI. Systemic and pulmonary arterial pressures were measured using the arterial cannula and the fiberoptic pulmonary artery catheter connected to two calibrated pressure transducers (PX-1X2; Baxter SA, Maurepas, France) positioned at the midaxillary line and recorded along with the EKG and tracheal pressure on a Gould ES 1000 recorder (Gould Instruments, Ballainvilliers, France). All pressures were measured at end-expiration. Cardiac output was measured using the thermodilution technique and a bedside computer, which allowed the recording of each thermodilution curve (Explorer; Baxter Healthcare). Systemic and pulmonary arterial blood samples were simultaneously withdrawn within 1 min after the measurements of cardiac output. Arterial pH, Pa_{O_2}, Pv_{O_2}, and Pa_{CO_2} were measured using an IL BGE blood gas analyzer (Instrumentation Laboratories, Paris, France). Hemoglobin concentration, and methemoglobin concentration, and arterial and mixed venous oxygen saturation (Sa_{O_2} and $S\bar{v}_{O_2}$) were measured using a calibrated OSM3 hemoximeter (Radiometer Copenhagen, Neuilly-Plaisance, France). Standard formulas were used to calculate cardiac index, true pulmonary shunt ($\dot{Q}s/\dot{Q}T$), oxygen delivery ($\dot{D}o_2$), and oxygen consumption ($\dot{V}o_2$).

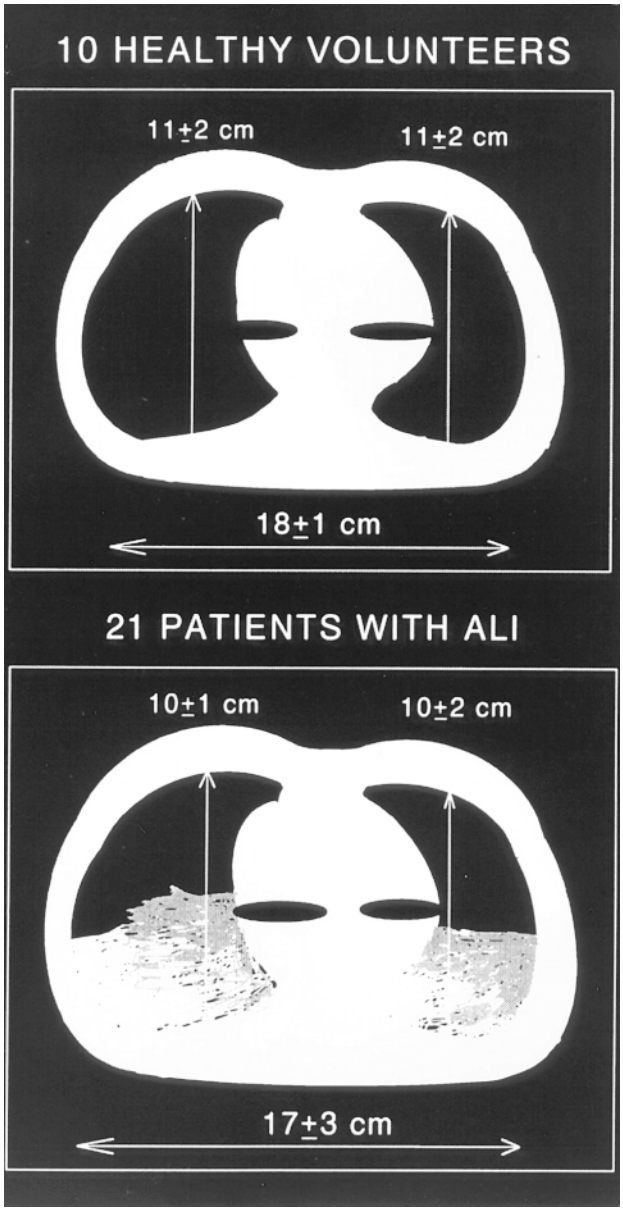

Figure 3. Anteroposterior and transverse dimensions of the lung measured at zero end-expiratory pressure at the level of the tracheal carina in the 10 healthy volunteers and the 21 patients with acute lung injury.

Respiratory Measurements

Expired CO_2 was measured using a nonaspirative calibrated 47210A infrared capnometer (Hewlett-Packard, Andover, MA) positioned between the proximal end of the endotracheal tube and the Y-piece of the ventilator and recorded on the Gould ES 1000. After simultaneously withdrawing an arterial blood sample, the ratio of alveolar dead space ($\dot{V}_{DA}$) to tidal volume (V_T) was calculated as:

$$\dot{V}_{DA}/V_T = 1 - (P_{ET_{CO_2}}/Pa_{CO_2}) \quad (1)$$

where $P_{ET_{CO_2}}$ is end tidal CO_2 measured at the plateau of the expired CO_2 curve.

Respiratory volume-pressure curves were obtained using the gross syringe technique (14) and opening pressure (Pop) was visually determined. Quasi-static respiratory compliance (Cst) was calculated by dividing the V_T of the patient by the corresponding airway pressure on the volume-pressure curve. In each individual patient, the PEEP value of 10 cm H_2O was always equal to or greater than Pop.

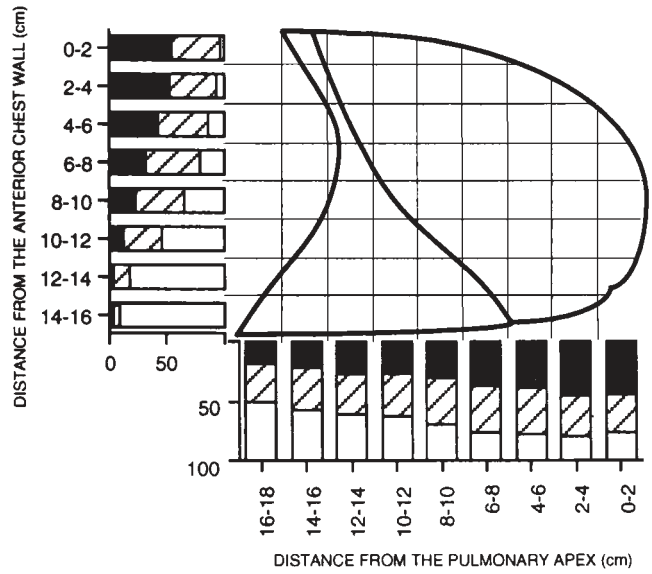

Figure 4. Distribution (expressed in percentage) of aerated (*closed part of bars*), poorly aerated (*hatched part of bars*), and nonaerated (*open part of bars*) lung areas along the anteroposterior and the cephalocaudal axis for the overall lung in ZEEP. Each *bar* represents the lung parenchyma located at a given distance (indicated in centimeters) from the anterior chest wall or from the pulmonary apex. Aerated lung decreases and nonaerated lung increases along the anteroposterior and cephalocaudal axis.

Statistical Analysis

Lung dimensions and volumes of upper and lower right and left lobes were compared between patients and healthy volunteers using Student's unpaired *t* test. Anteroposterior and cephalocaudal distributions of aerated, poorly aerated, and nonaerated lung parenchyma (expressed in percentage of lobar lung volume) were compared between upper and lower lobes by a two-way analysis of variance for one grouping and one within factor. The correlation between the resting volume of the upper and lower lobes and PEEP-induced alveolar recruitment at the lobar level was tested by linear regression analysis. The effects of PEEP on hemodynamic and respiratory variables were compared in nonrecruiter and recruiter patients by a two-way analysis of variance for one grouping and one within factor. All data are expressed as mean ± SD. The significance level was fixed at 0.05.

RESULTS

Patients

There were 16 male and five female patients (55 ± 17 yr of age). Ten patients were admitted because of complications after surgery: cardiovascular (n = 6), orthopedic (n = 1), urologic (n = 1), maxillofacial (n = 1), and neurosurgical (n = 1). Nine patients were admitted for multiple trauma, one for acute pancreatitis and one for a ruptured cerebral aneurysm. Seven of the nine patients with multiple trauma had to have surgery (abdominal surgery, n = 1; orthopedic surgery, n = 6). Clinical and cardiorespiratory characteristics recorded on the day of inclusion are presented in Tables 1 and 2. The mean delay between the onset of ALI and CT scan was 5 ± 5 d. Overall mortality was 38%. Mean durations of the stay in the ICU and of mechanical ventilation were 39 ± 33 d and 36 ± 22 d, respectively. As a mean, patients were severely hypoxemic, with a Pa_{O_2} measured at FI_{O_2} 1 and ZEEP of 104 ± 60 mm Hg and a true shunt value of 44 ± 13%. Furthermore, they had pulmonary hypertension (mean pulmonary artery pressure

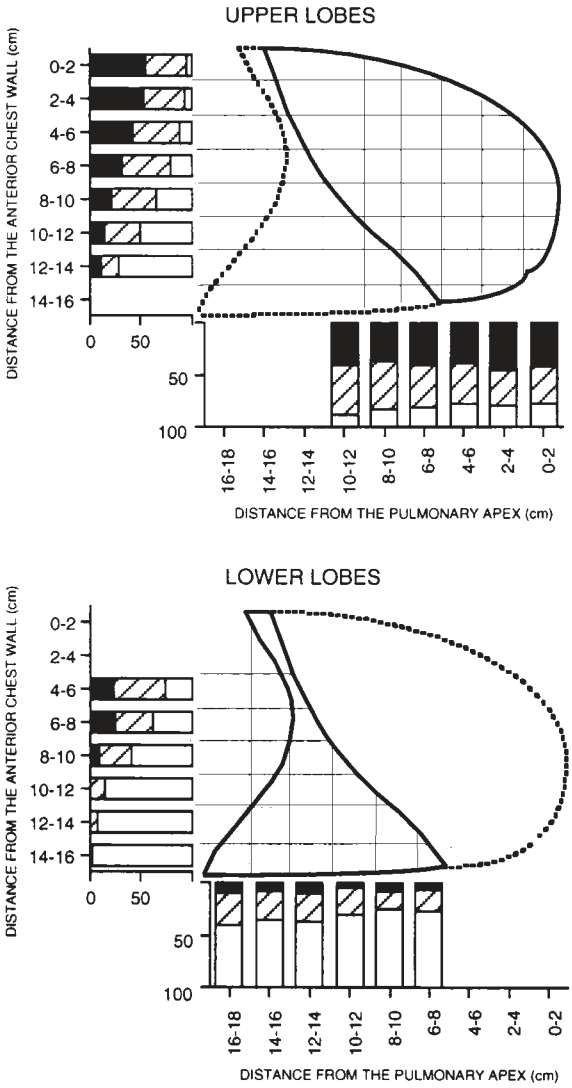

Figure 5. Distribution (expressed in percentage) along the anteroposterior and cephalocaudal axis of aerated (*closed part of bars*), poorly aerated (*hatched part of bars*), and nonaerated (*open part of bars*) lung areas of upper and lower lobes analyzed separately. Each *bar* represents the lung parenchyma located at a given distance (indicated in centimeters) from the anterior chest wall or from the pulmonary apex. Aerated lung areas are mainly located in the nondependent regions, whereas nonaerated lung areas are located in dependent regions. Between the fourth and the fourteenth centimeter from the anterior chest wall, percentage of each zone is similar in upper and lower lobes. No cephalocaudal gradient of aerated and nonaerated lung is observed for both upper and lower lobes. For a given distance from the pulmonary apex, percentage of nonaerated lung areas is always greater and percentage of aerated lung areas smaller in lower than in upper lobes.

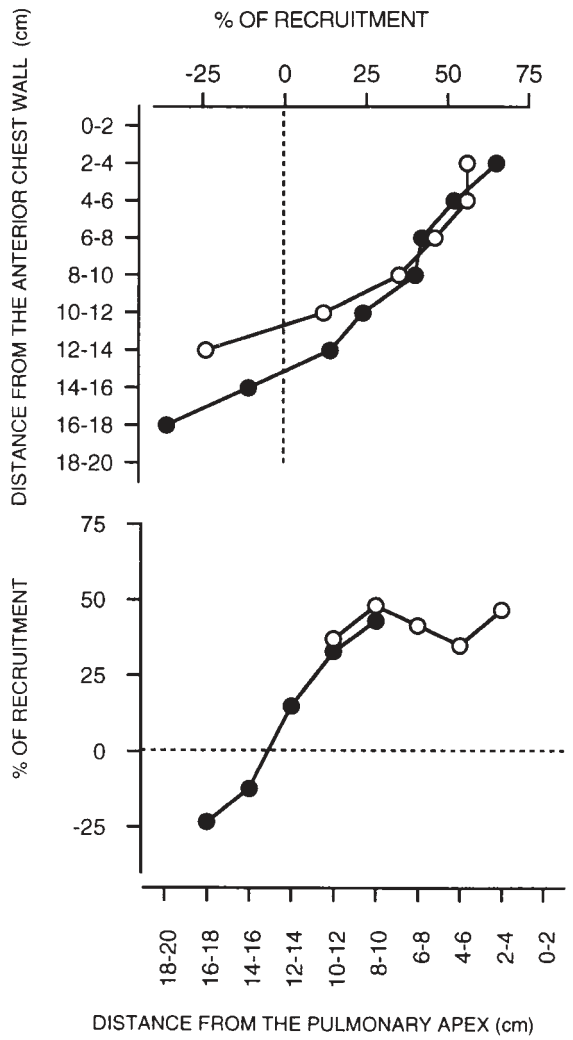

Figure 6. Percentage of PEEP-induced alveolar recruitment of a given nonaerated area according to its location on the anteroposterior (*upper panel*) and cephalocaudal axis (*lower panel*) for the upper lobes (*open circles*) and the lower lobes (*closed circles*). The *dashed line* indicates the cut-off between PEEP-induced alveolar recruitment and derecruitment. PEEP-induced alveolar recruitment predominantly occurs in nondependent and cephalad lung regions.

$[\overline{Ppa}]$ = 32 ± 11 mm Hg) and increased dead space (39 ± 11%). Septic shock was associated with ALI in four patients.

There were seven male and three female healthy volunteers (37 ± 16 yr of age). The mean heights and weights of the patients and healthy volunteers were similar (173 ± 8 versus 172 ± 6 cm and 70 ± 8 versus 66 ± 10 kg).

Dimensions of the Thorax

As shown in Figure 1, the cephalocaudal dimensions of right and left lung were significantly reduced in patients with ALI as compared with those in healthy volunteers (both $p < 0.05$). In patients with ALI, the ratio of cephalocaudal dimension/body height was 7.9 ± 2.3% on the right and 8.5 ± 2.4% on the left. In healthy volunteers, corresponding values were 9.8 ± 2.3% and 11.0 ± 0.7% (both $p < 0.01$). This finding is illustrated in Figure 2, which shows sagittal CT reconstruction of the right lungs of a patient and of a healthy volunteer. Cephalocaudal dimensions were similar in patients with (148 ± 21 and 157 ± 19 mm for the right and left lung, n = 6) and without (142 ± 27 and 155 ± 28 mm, respectively, n = 15) a surgical thoracic or abdominal incision. As shown in Figure 3, anteroposterior and transverse diameters of the lung measured at the level of the tracheal carina were not different in patients with ALI from those in healthy volunteers.

Loss of Lung Volume in ZEEP Conditions

Total lung volume (gas plus tissue) in ZEEP of patients with ALI was reduced by 27% as compared with healthy volun-

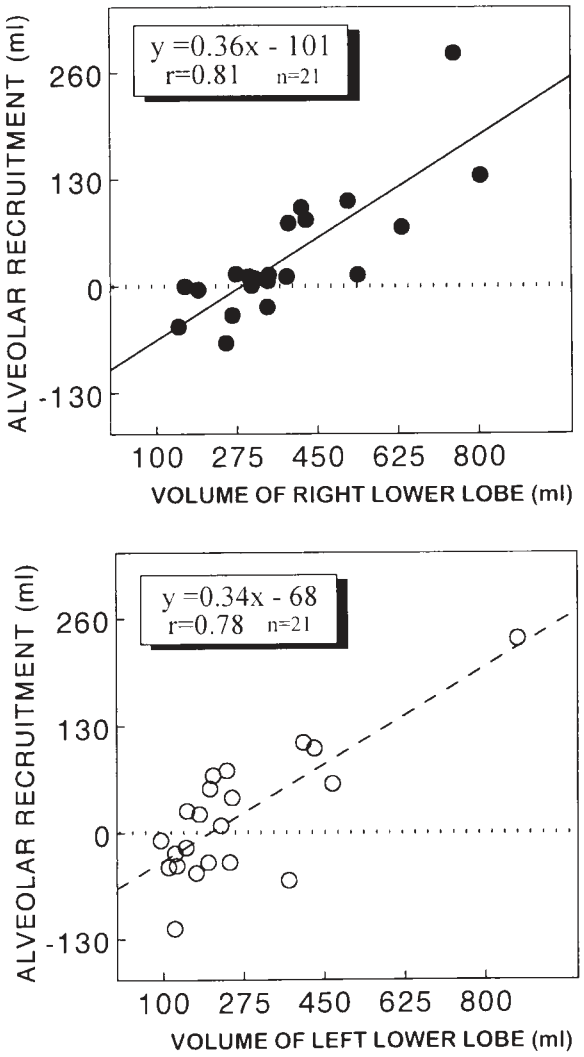

Figure 7. Correlation between the resting volume in ZEEP- and PEEP-induced changes in the volume of nonaerated lung parenchyma of right lower lobes (*upper panel*, *closed circles*) and of left lower lobes (*lower panel*, *open circles*) from the 21 patients. Both correlations were significant ($p < 0.001$). The *horizontal dashed line* indicates the cutoff between recruitment and derecruitment.

teers (2,777 ± 1,001 ml versus 3,793 ± 647 ml, $p < 0.01$). Volume of pleural fluid was 287 ± 300 ml. As shown in Figure 1, left upper and lower lobes were significantly smaller than the corresponding right lobes ($p < 0.001$). Resting volumes of upper lobes were significantly greater than resting volumes of lower lobes ($p < 0.0001$). The reduction in the overall lung volume and in the volume of lower lobes was similar in patients with a lung injury severity score (LISS) below and above 2.5. When considering only normally and poorly aerated lung areas, volumes of upper and lower lobes were 83 and 17% of the corresponding volumes measured in healthy volunteers. When considering both lungs, 31 ± 27% of the lung parenchyma was normally aerated, 36 ± 23% was poorly aerated, and 33 ± 14% was nonaerated.

The distribution of the percentage of aerated, poorly aerated, and nonaerated lung areas along the anteroposterior and the cephalocaudal axis is shown in Figure 4. Aerated lung areas were predominantly located in the most anterior and cephalad regions, whereas nonaerated lung areas were located in the most posterior and caudal regions. The distribution of gas and tissue along the anteroposterior and cephalocaudal axis for upper and lower lobes analyzed separately is shown in Figure 5. The increase in the percentage of nonaerated lung along the anteroposterior axis was similar between upper and lower lobes. For a given distance from the pulmonary apex, the proportion of aerated lung was always lower and the proportion of nonaerated lung was always higher in lower than in upper lobes. For both upper and lower lobes, no cephalocaudal gradient in the distribution of gas and tissue was observed, suggesting that upper lobes remain better aerated than do lower lobes, essentially because of their nondependent anatomic situation.

Factors Influencing PEEP-induced Alveolar Recruitment

As shown in Figure 6, PEEP-induced alveolar recruitment in upper and lower lobes depended on an anteroposterior gradient and was predominantly observed in nondependent lung regions. In the most dependent parts of the lung, the amount of nonaerated tissue increased with PEEP, suggesting a PEEP-induced alveolar derecruitment. A cephalocaudal gradient of PEEP-induced alveolar recruitment was also observed in lower lobes, the most cephalad regions recruiting better than the caudal regions. Derecruitment was observed in lung regions that were the closest to the diaphragmatic cupola.

As shown in Figure 7, a significant correlation was found between the resting volume of the right and left lower lobes and PEEP-induced lobar alveolar recruitment ($p < 0.001$). As illustrated in Figures 8 and 9, the higher the resting volume of lower lobes, the higher was the PEEP-induced alveolar recruitment.

Effects of PEEP-induced Alveolar Recruitment on Cardiorespiratory Parameters

Patients were classified into two groups according to the existence ("recruiter") or the absence ("nonrecruiter") of PEEP-induced alveolar recruitment on spiral CT scan. PEEP-induced alveolar recruitment could be demonstrated in 13 patients. Resting volumes of lower lobes (gas plus tissue) were significantly higher in recruiter than in nonrecruiter patients (1,074 ± 492 ml versus 699 ± 125 ml, $p < 0.01$), whereas resting volumes of upper lobes were similar between groups (1,965 ± 956 versus 1,649 ± 318 ml; NS). Respiratory parameters of both groups are summarized in Table 3. In nonrecruiters, PEEP had no effect on Pa_{O_2}, $S\bar{v}_{O_2}$, $P\bar{v}_{O_2}$, $\dot{Q}s/\dot{Q}T$, $\dot{D}_{O_2}$, $\dot{V}_{O_2}$, $P_{ET}CO_2$, Pa_{CO_2}, and $\dot{V}_{DA}/V_T$. In recruiters, PEEP significantly increased Pa_{O_2} (51 ± 45%), and significantly decreased $\dot{Q}s/\dot{Q}T$ (−14 ± 14%). PEEP increased right atrial pressure and capillary wedge pressure in both groups. PEEP had no effect on heart rate, cardiac output, mean arterial pressure, mean pulmonary artery pressure, or systemic and pulmonary vascular resistance.

DISCUSSION

This study demonstrates three original findings. In patients with severe acute lung injury: (*1*) there is a reduction of overall lung volume (gas plus tissue) predominating in the lower lobes; (*2*) nonaerated lung regions are distributed not only along an anteroposterior axis, as previously shown (9), but also along a cephalocaudal axis; (*3*) in lower lobes, alveolar recruitment induced by a PEEP level of 10 cm H_2O is correlated with the resting volume and decreases along the cephalocaudal axis. These results were observed in patients showing the characteristic features of severe respiratory failure, i.e., low respiratory compliance, marked hypoxemia, increased pulmo-

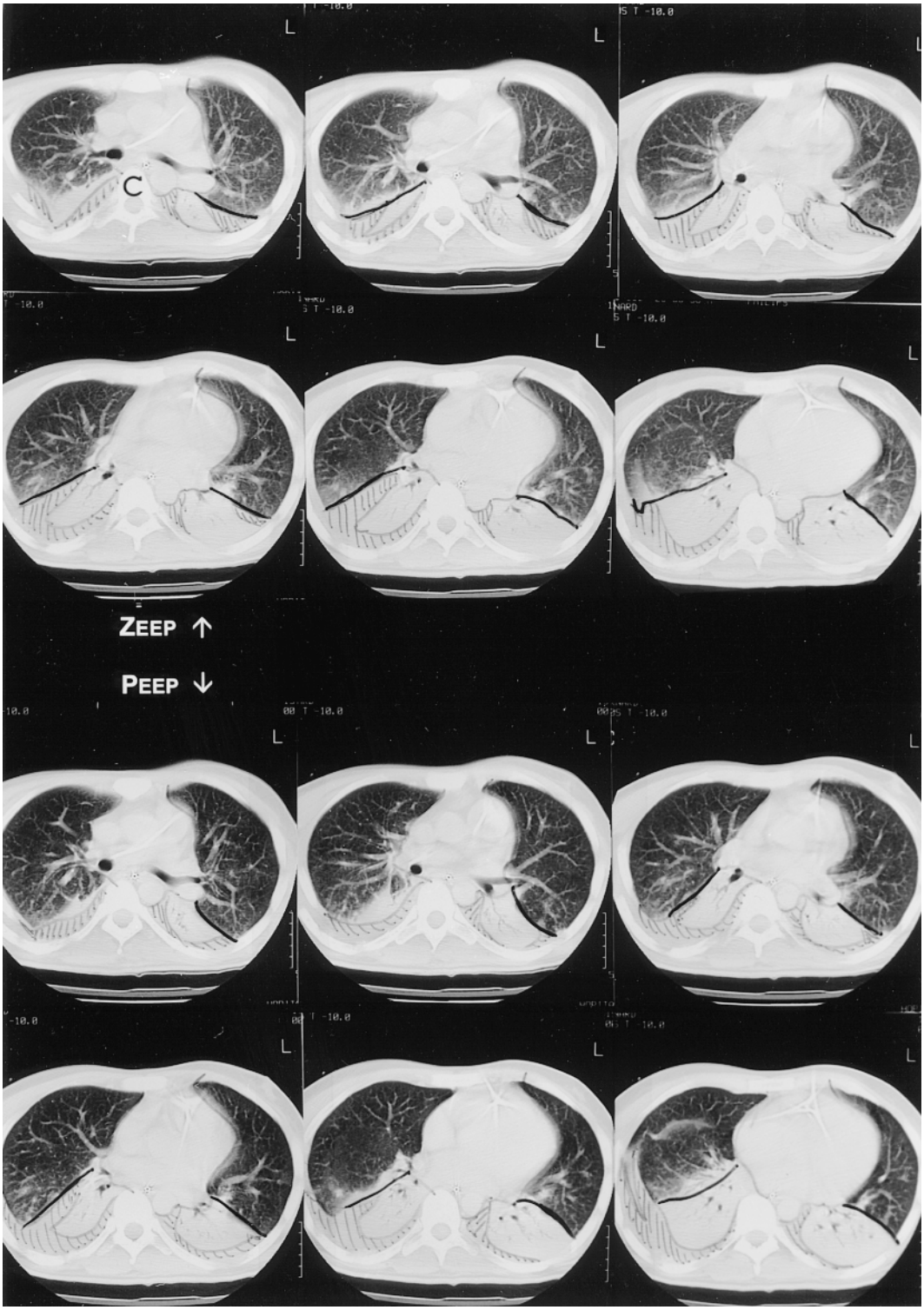

Figure 8. CT scan of a nonrecruiter patient (Patient 14) showing a marked reduction in the volume of lower lobes and no alveolar recruitment with PEEP. The *black line* represents the position of the major fissura. The *hatched areas* represent the pleural fluid. The characteristics of this patient are shown in Tables 1 and 2.

nary artery pressure, and alveolar dead space. Nearly two thirds of the patients had a LISS equal or above 2.5, and the vast majority of them had a Pa_{O_2}/FI_{O_2} ratio below 200 mm Hg. In addition, the mortality rate was 38%, and the mean duration of mechanical ventilation exceeded 1 mo.

Reduction of FRC (aerated lung volume) is a very common finding in patients with the acute respiratory distress syndrome (15–17). An accurate assessment of overall lung volume loss (aerated and nonaerated lung volume) requires tomodensitometric measurements. A single CT section obtained

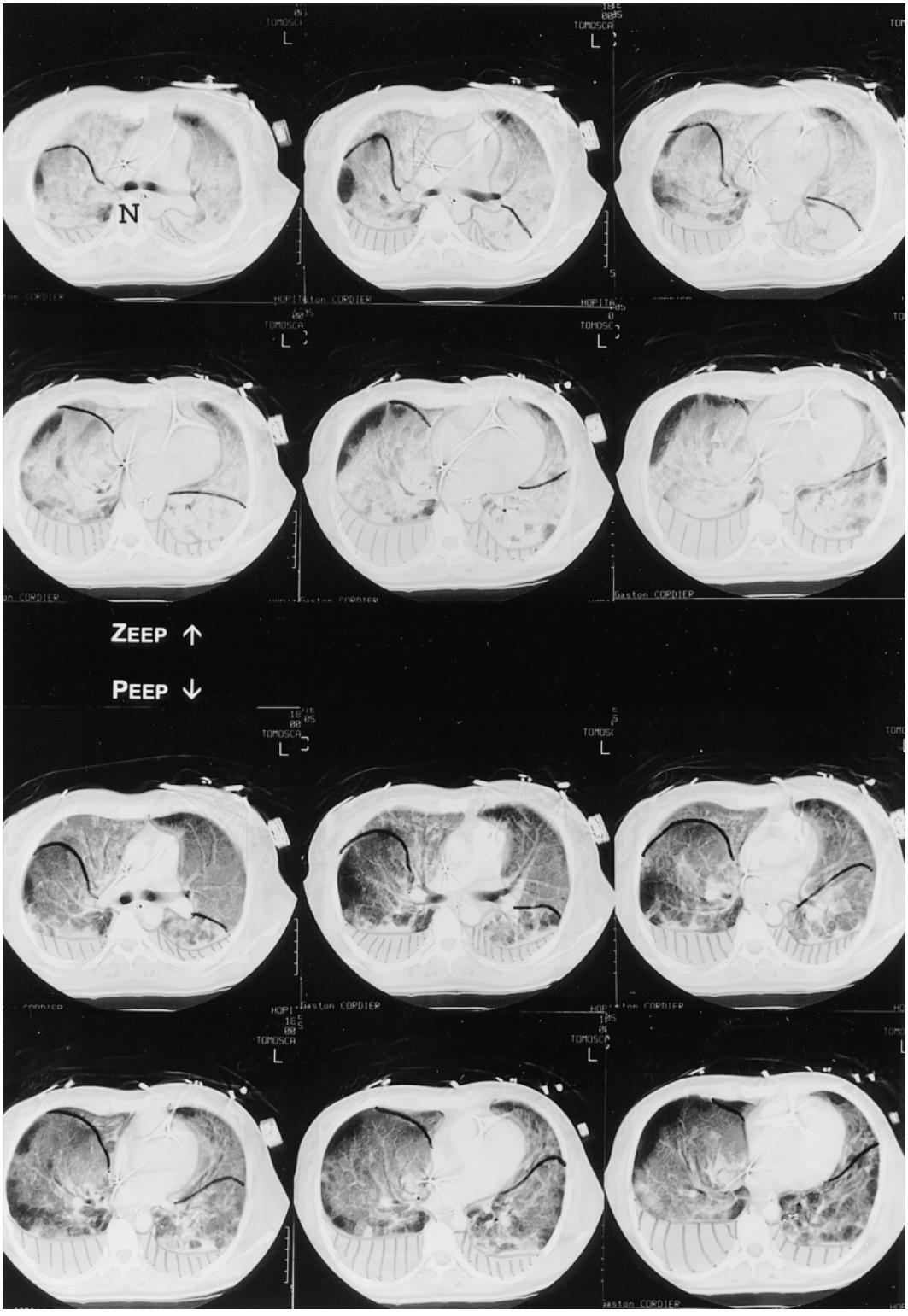

Figure 9. CT scan of a recruiter patient (Patient 21) showing no reduction in the volume of lower lobes and a marked alveolar recruitment with PEEP. The *black line* represents the position of the major fissura. The *hatched areas* represent the pleural fluid. The characteristics of this patient are shown in Tables 1 and 2.

with a conventional scanner allows a bidimensional assessment of lung dimensions along the anteroposterior and transverse axis and the measurement of a very small fraction of the lung volume (6, 8, 10, 18, 19). Multiple and contiguous CT sections obtained during a short apnea with a spiral CT scanner offer a tridimensional approach of lung dimensions including the cephalocaudal axis. It also allows the measurement of the entire lung volume and the assessment of regional volumes. Using the tomodensitometric analysis, we found, in healthy volunteers lying supine, a mean end-expiratory lung volume of

TABLE 3

RESPIRATORY AND HEMODYNAMIC PARAMETERS IN ZEEP AND PEEP 10 cm H_2O IN PEEP RECRUITER AND IN PEEP NONRECRUITER PATIENTS*

	PEEP Recruiters		PEEP Nonrecruiters	
	ZEEP	PEEP	ZEEP	PEEP
Pa_{O_2}, mm Hg	98 ± 56	148 ± 93†	110 ± 57	125 ± 79
$S\bar{v}_{O_2}$, %	63 ± 10	65 ± 9	59 ± 10	63 ± 10
$P\bar{v}_{O_2}$, mm Hg	37 ± 6	41 ± 10	38 ± 8	38 ± 11
$\dot{Q}s/\dot{Q}_T$, (%)	44 ± 12	37 ± 8†	45 ± 8	39 ± 9
$\dot{D}o_2$, ml/min/m^{-2}	398 ± 148	430 ± 133	401 ± 139	393 ± 141
$\dot{V}o_2$,ml/min/m^{-2}	123 ± 31	133 ± 34	135 ± 32	132 ± 34
$P_{ET_{CO_2}}$, mm Hg	26 ± 6	28 ± 5	29 ± 5	29 ± 5
Pa_{CO_2}, mm Hg	46 ± 8	45 ± 7	43 ± 6	42 ± 5
$\dot{V}_{DA}/\dot{V}_T$, %	42 ± 12	37 ± 8	32 ± 8	30 ± 8
HR, beats/min	100 ± 16	97 ± 17	93 ± 15	95 ± 17
CI, L/min/m^2	3.5 ± 1.0	3.7 ± 1.2	3.9 ± 1.1	3.6 ± 1.3†
$\overline{Pa}$, mm Hg	79 ± 15	81 ± 11	81 ± 12	80 ± 10
SVRI, dyn/s/cm^{-5}/m^2	1,789 ± 951	1,765 ± 1,005	1,591 ± 981	1,734 ± 1,109
$\overline{Ppa}$, mm Hg	34 ± 10	36 ± 8	30 ± 11	30 ± 9
PVRI, dyn/s/cm^{-5}/m^2	639 ± 490	623 ± 392	545 ± 574	506 ± 458
Ppcw, mm Hg	10 ± 4	11 ± 5†	8 ± 5	10 ± 5†
P_{RA}, mm Hg	9 ± 4	10 ± 5†	8 ± 5	9 ± 6†

Definition of abbreviations: CI = cardiac index; $\dot{D}o_2$ = oxygen delivery index; HR = heart rate; $\overline{Pa}$ = mean arterial pressure; $P_{ET_{CO_2}}$ = end-tidal CO_2; $\overline{Ppa}$ = mean pulmonary artery pressure; Ppcw = pulmonary capillary wedge pressure; P_{RA} = right atrial pressure; $P\bar{v}_{O_2}$ = mixed venous oxygen pressure; PVRI = pulmonary vascular resistance; $\dot{Q}s/\dot{Q}_T$ = pulmonary shunt; SVRI = systemic vascular resistance; $S\bar{v}_{O_2}$ = mixed venous oxygen saturation; $\dot{V}_{DA}/\dot{V}_T$ = alveolar dead space to tidal volume ratio; $\dot{V}o_2$ = oxygen consumption index.

* Values are means ± SD.

† $p < 0.05$ as compared with ZEEP.

3,793 ± 647 ml, whereas standard formulas (20) were predicting a theoretical FRC of 3,159 ± 335 ml ($p < 0.01$). This difference is likely related to the fact that the tomodensitometric method measures not only the alveolar volume but also the volume of the pulmonary vessels and tissular structures. The present study is the first demonstration that total lung volume—including aerated and nonaerated lung parenchyma—is markedly reduced in patients with acute lung injury. Total lung volume of patients with acute lung injury was reduced by 27% as compared with that in healthy volunteers of similar height and weight. The loss of overall volume was predominantly observed in the lower lobes where the volume averaged 48% of that of the healthy volunteers. Interestingly, these changes were similar in patients with a LISS below or above 2.5. In contrast, the volume of upper lobes in healthy volunteers was similar to that of the patients. Reduction in the volume of the lower lobes was associated with a 15% decrease of the cephalocaudal dimension of the right and with an 18% decrease of the cephalocaudal dimension of the left lung. Anteroposterior and transverse dimensions were similar in healthy volunteers and patients, as previously reported by Pelosi and colleagues (9). On the basis of this finding, these investigators hypothesized that the overall lung volume was not reduced in patients with acute lung injury, likely because the decrease in aerated lung volume was counterbalanced by an equivalent increase in nonaerated lung volume. The present study does not confirm this assumption and shows a decrease in overall lung volume along the cephalocaudal axis, a dimension that could not be measured in the study of Pelosi and colleagues where a single CT section was analyzed.

The upward shift of the diaphragm that we observed in patients with acute lung injury could be either the cause or the consequence of the reduction of volume of the lower lobes. Diaphragmatic function is impaired after abdominal and thoracic surgery (21, 22). Nine of the 21 patients included in this study had operative procedures through thoracic or abdominal approaches, and a diaphragmatic dysfunction was likely present in the immediate postoperative period, thereby contributing to atelectasis formation in lower lobes. General anesthesia and muscle relaxation also markedly interferes with diaphragmatic function by suppressing diaphragmatic tonus and active contraction (23). Agostini and colleagues (24, 25) reported a dramatic reduction in juxtadiaphragmatic transpulmonary pressure after anesthesia and muscle paralysis in experimental animals, resulting in partial collapse of lower lobes (24). Interestingly, a certain degree of transpulmonary pressure gradient could be reestablished at the lung base by removing the intestine mass from the abdominal cavity, suggesting that abdominal pressure was playing a key role. Confirming these experimental results, Froese and Bryan (26) showed in the 1970s that anesthesia and paralysis alone could induce an upward shift in the end-expiratory position of the diaphragm. Using fast computed tomography, Warner and colleagues (27) confirmed this result. They observed, similar to the observations of Froese and Bryan (26), that the cephalad displacement of the diaphragm occurred predominantly in posterior regions, likely because the abdominal pressure is greater in these regions. Because all the patients of the present study were anesthetized and paralyzed, it is likely that the observed reduction in lung volume of lower lobes was at least related to a decrease in juxtadiaphragmatic transpulmonary pressure induced by increased abdominal pressure and general anesthesia.

An uneven distribution of aerated, poorly aerated, and nonaerated lung parenchyma was observed. Upper lobes remained predominantly aerated, whereas lower lobes appeared for the most part nonaerated. When present in the upper lobes, lung hyperdensities were predominantly observed in dependent lung areas, whereas the few aerated lung regions observed in the lower lobes were preferentially found in nondependent areas as previously described (3, 6, 28). To explain the dependency of nonaerated lung along an anteroposterior axis, Pelosi and colleagues (9) proposed an elegant hypothesis: the diffuse increase in alveolocapillary permeability causes an evenly distributed interstitial edema that increases lung weight

along the anteroposterior axis, which in turn causes compression atelectasis of the dependent lung regions through a decrease in the transpulmonary pressure. To support their hypothesis, they demonstrated that superimposed hydrostatic pressure increases according to an anteroposterior gradient in patients with acute lung injury (9). Further confirmation was obtained by Sandiford and colleagues (29) who found an increase in the radiologic density along an anteroposterior gradient in patients with acute lung injury although the increased pulmonary vascular permeability assessed by positron emission tomography was evenly distributed. Experimentally, oleic-acid-induced lung injury was also shown to induce a dependent increase in lung density in dogs (30). We found an increase in lung tissue density not only along an anteroposterior axis, but also along a cephalocaudal axis. Contrasting with the anteroposterior dependency, cephalocaudal dependency was observed on the overall lung but not on upper or lower lobes when they were analyzed separately. This difference suggests that, besides the decrease in transpulmonary pressure caused by an increased abdominal pressure, an anatomic factor is also implicated in the cephalocaudal distribution of lung hyperdensities.

PEEP of 10 cm H_2O significantly increased Pa_{O_2}, and decreased $\dot{Q}s/\dot{Q}T$ only in patients demonstrating scanographic alveolar recruitment. The present study supports the findings of Gattinoni's group that in acute lung injury, PEEP-induced alveolar recruitment decreases along the anteroposterior axis, the nondependent parts of the lung recruiting more than the dependent parts. In this respect, upper and lower lobes behave similarly, the only determinant of PEEP-induced alveolar recruitment being the distance from the anterior chest wall. We also observed, similar to Gattinoni and colleagues (10), that a PEEP of 10 cm H_2O slightly increased the amount of noninflated tissue in the most dependent parts of the lung, suggesting that PEEP may be associated with alveolar derecruitment related to local compression atelectasis by overdistended upper lobes. In lower lobes, PEEP-induced alveolar recruitment decreased along the cephalocaudal axis. Two CT scan studies have recently shown that, besides gravity, atelectasis secondary to anesthesia also depends upon a cephalocaudal gradient, the caudal regions being more atelectatic than the cephalad regions (31, 32). In the present study, PEEP-induced alveolar recruitment in lower lobes was linearly correlated with resting volume of lower lobes, whereas such a correlation was not observed in upper lobes. The opening pressure of a passively collapsed lung when transpulmonary pressure is zero is known to be near 30 cm H_2O (33), a pressure much higher than the pressure required to overcome the pressure gradient along the anteroposterior axis that was calculated at 11 cm H_2O by Pelosi and colleagues (9). Passive collapse of lower lobes related to a diminution of juxtadiaphragmatic transpulmonary pressure likely results in an increase in regional opening pressure, which precludes any significant PEEP-induced alveolar recruitment. Thirty percent of patients with acute lung injury do not respond to PEEP (34) or even deteriorate after PEEP implementation (34, 35). One possible explanation for the unforeseeable effect of PEEP might be related to the amount of passive atelectasis that is associated with acute respiratory failure. According to our data, the resting volume of the lower lobes markedly influences the response to PEEP.

In conclusion, this study has demonstrated that the marked reduction of lung volume observed in acute lung injury predominates in lower lobes and influences PEEP-induced alveolar recruitment. Reduction in lung volume increases along the anteroposterior and the cephalocaudal axis, suggesting two causative mechanisms: an increase in lung weight related to acute lung injury and a passive collapse of lower lobes associated with an upward shift of the diaphragm related to muscle paralysis and an increase in intra-abdominal pressure. As a consequence, PEEP-induced alveolar recruitment predominantly occurs in nondependent and cephalad lung regions.

References

1. Hylkema, B. S., P. Barkmeijer-Degenhart, T. W. Van der Mark, R. Peset, and H. J. Sluiter. 1982. Measurement of functional residual capacity during mechanical ventilation for acute respiratory failure. *Chest* 81:27–30.
2. East, T. D., P. J. M. Wortelboer, E. Van Ark, F. H. Bloem, L. Peng, N. L. Pace, R. O. Crapo, D. Drews, and T. P. Clemmer. 1990. Automated sulfur hexafluoride washout functional residual capacity measurement system for any mode of mechanical ventilation as well as spontaneous respiration. *Crit. Care Med.* 18:84–91.
3. Gattinoni, L., D. Mascheroni, A. Torresin, R. Marcolin, R. Fumagalli, S. Vesconi, G. Rossi, F. Rossi, S. Baglioni, F. Bassi, F. Nastri, and A. Pesenti. 1986. Morphological response to positive end-expiratory pressure in acute respiratory failure. Computerized tomography study. *Intensive Care Med.* 12:137–142.
4. Macnaughton, P. D., and T. W. Evans. 1994. Measurement of lung volume and $D_{L_{CO}}$ in acute respiratory failure. *Am. J. Respir. Crit. Care Med.* 150:770–775.
5. Ibanez, J., J. M. Raurich, and S. G. Moris. 1983. Measurement of functional residual capacity during mechanical ventilation. Comparison of a computerized open nitrogen washout method with a closed helium dilution method. *Intensive Care Med.* 9:91–93.
6. Gattinoni, L., A. Pesenti, L. Avalli, F. Rossi, and M. Bombino. 1987. Pressure-volume curve of total respiratory system in acute respiratory failure: computed tomographic scan study. *Am. Rev. Respir. Dis.* 136: 730–736.
7. Maunder, R. J., W. P. Shuman, J. W. McHugh, S. I. Marglin, and J. Butler. 1986. Preservation of normal lung regions in the adult respiratory distress syndrome. *J.A.M.A.* 255:2463–2465.
8. Gattinoni, L., L. D'andrea, P. Pelosi, G. Vitale, A. Pesenti, and R. Fumagalli. 1993. Regional effects and mechanism of positive end-expiratory pressure in early adult respiratory distress syndrome. *J.A.M.A.* 269:2122–2127.
9. Pelosi, P., L. D'andrea, A. Pesenti, and L. Gattinoni. 1994. Vertical gradient of regional lung inflation in adult respiratory distress syndrome. *Am. J. Respir. Crit. Care Med.* 149:8–13.
10. Gattinoni, L., P. Pelosi, S. Crotti, and F. Valenza. 1995. Effects of positive end-expiratory pressure on regional distribution of tidal volume and recruitment in adult respiratory distress syndrome. *Am. J. Respir. Crit. Care Med.* 151:1807–1814.
11. Lu, Q., E. Mourgeon, J. D. Law-Koune, S. Roche, C. Vézinet, L. Abdenour, E. Vicaut, L. Puybasset, M. Diaby, P. Coriat, and J. J. Rouby. 1995. Dose-response of inhaled NO with and without intravenous almitrine in adult respiratory distress syndrome. *Anesthesiology* 83: 929–943.
12. Puybasset, L., T. E. Stewart, J. J. Rouby, P. Cluzel, E. Mourgeon, M. F. Belin, M. Arthaud, C. Landault, and P. Viars. 1994. Inhaled nitric oxide reverses the increase in pulmonary vascular resistance induced by permissive hypercapnia in patients with ARDS. *Anesthesiology* 80: 1254–1267.
13. Puybasset, L., J. J. Rouby, E. Mourgeon, P. Cluzel, J. D. Law-Koune, T. Stewart, C. Devilliers, Q. Lu, S. Roche, P. Kalfon, E. Vicaut, and P. Viars. 1995. Factors influencing cardiopulmonary effects of inhaled nitric oxide in acute respiratory failure. *Am. J. Respir. Crit. Care Med.* 152:318–328.
14. Matamis, D., F. Lemaire, A. Harf, C. Brun-Buisson, J. C. Ansquer, and G. Atlan. 1984. Total respiratory pressure-volume curves in the adult respiratory distress syndrome. *Chest* 86:58–66.
15. Falke, K. J., H. Pontoppidan, A. Kumar, D. E. Leith, B. Geffin, and M. B. Laver. 1972. Ventilation with end-expiratory pressure in acute lung disease. *J. Clin. Invest.* 51:2315–2323.
16. Suter, P. M., B. F. Fairley, and M. D. Isenberg. 1975. Optimum end-expiratory airway pressure in patients with acute pulmonary failure. *N. Engl. J. Med.* 292:284–289.
17. Petty, T. L., G. W. Silvers, G. W. P. Paul, and R. E. S. Stanford. 1979. Abnormalities in lung elastic properties and surfactant function in adult respiratory distress syndrome. *Chest* 75:571–574.
18. Gattinoni, L., P. Pelosi, G. Vitale, A. Pesenti, L. D'andrea, and D. Mas-

cheroni. 1991. Body position changes redistribute lung computed tomographic density in patients with acute respiratory failure. *Anesthesiology* 74:15–23.
19. Gattinoni, L., P. Pelosi, A. Pesenti, L. Bazzi, G. Vitale, A. Moretto, A. Crespi, and M. Tagliabue. 1991. CT scan in ARDS: clinical and physiopathological insights. *Acta Anaesthesiol. Scand.* 35(Suppl. 95):87–96.
20. Quanjer, P. H., G. J. Tammeling, J. E. Cotes, O. F. Pedersen, R. Peslin, and J. C. Yernault. 1993. Lung volume and forced ventilatory flows. *Eur. Respir. J.* 6:5–40.
21. Ford, G. T., W. A. Whitelaw, T. W. Rosenal, P. J. Cruse, and C. A. Guenter. 1983. Diaphragm function after upper abdominal surgery. *Am. Rev. Respir. Dis.* 127:431–436.
22. Simmoneau, G., A. Vivien, R. Sartene, F. Kunstlinger, K. Samii, Y. Noviant, and P. Duroux. 1983. Diaphragm dysfunction induced by upper abdominal surgery: role of postoperative pain. *Am. Rev. Respir. Dis.* 128:899–903.
23. Clergue, F., N. Viires, P. Lemesle, M. Aubier, P. Viars, and R. Pariente. 1986. Effect of halothane on diaphragmatic muscle function in pentobarbital-anesthetized dogs. *Anesthesiology* 64:181–187.
24. Agostini, E., E. D'angelo, and M. V. Bonanni. 1970. Topography of pleural surface pressure above resting volume in relaxed animals. *J. Appl. Physiol.* 29:297–306.
25. Agostini, E., E. D'angelo, and M. V. Bonanni. 1970. The effect of the abdomen on the vertical gradient of pleural surface pressure. *Respir. Physiol.* 8:332–346.
26. Froese, A. B., and A. C. Bryan. 1974. Effects of anesthesia and paralysis on diaphragmatic mechanics in man. *Anesthesiology* 41:242–254.
27. Warner, D. O., M. A. Warner, and E. L. Ritman. 1995. Human chest wall function while awake and during anesthesia: I. Quiet breathing. *Anesthesiology* 82:6–19.
28. Gattinoni, L., A. Pesenti, M. Bombino, S. Baglioni, M. Rivolta, G. Rossi, F. Rossi, R. Marcolin, D. Mascheroni, and A. Torresin. 1988. Relationships between lung computer tomographic density, gas exchange, and PEEP in acute respiratory failure. *Anesthesiology* 69:824–832.
29. Sandiford, P., M. A. Province, and D. P. Schuster. 1995. Distribution of regional density and vascular permeability in the adult respiratory distress syndrome. *Am. J. Respir. Crit. Care Med.* 151:737–742.
30. Slutsky, R. A., S. Long, W. W. Peck, C. B. Higgins, and R. Mattrey. 1984. Pulmonary density distribution in experimental noncardiac canine pulmonary edema evaluated by computed transmission tomography. *Invest. Radiol.* 19:168–173.
31. Reber, A., G. Engberg, B. Sporre, L. Kviele, H.-U. Rothen, G. Wegenius, U. Nylund, and G. Hedenstierna. 1996. Volumetric analysis of aeration in the lungs during general anaesthesia. *Br. J. Anaesth.* 76: 760–766.
32. Warner, D. O., M. A. Warner, and E. L. Ritman. 1996. Atelectasis and chest wall shape during halothane anesthesia. *Anesthesiology* 85:49–59.
33. Greaves, I. A., J. Hildebrandt, and F. G. Hoppin. 1986. Micromechanics of the lung. *In* P. T. Macklem and J. Mead, editors. Handbook of Physiology. American Physiological Society, Bethesda, MD. 217–231.
34. Horton, W. G., and F. W. Cheney. 1975. Variability of effect of positive end-expiratory pressure. *Arch. Surg.* 110:395–398.
35. Kanarek, D. J., and D. C. Shannon. 1975. Adverse effect of positive end-expiratory pressure on pulmonary perfusion and arterial oxygenation. *Am. Rev. Respir. Dis.* 112:457–459.